J. Earth Planet. Sci. Nagoya Univ., Vol. 43, 49 to 65, 1996

A preliminary CHIME age determination of monazites from metamorphic and granitic rocks in the Gyeonggi Massif, Korea

Deung-Lyong CHO*, Kazuhiro SUZUKI, Mamoru ADACHI** and Ueechan CHWAE***

**Geology Division, Korea Institute of Geology, Mining and Materials, 30 Kajeong-Dong, Yuseong-ku, Daejeon, 305-350, Korea*
***Department of Earth and Planetary Sciences, Graduate School of Science, Nagoya University, Nagoya 461-01, Japan*
(Received November 1, 1996 / Accepted November 29, 1996)

ABSTRACT

The CHIME (Chemical Th-U-Total Pb isochron method) dating was carried out for monazites from kyanite-staurolite-garnet schist of the Yeoncheon Group (Cheolwon area), and from sillimanite-garnet gneiss and two-mica granite in the central Gyeonggi Gneiss Complex (Hwacheon area). Monazites from the kyanite-staurolite-garnet schist yield an age of 255±8 Ma, and date the time of the regional metamorphism for the early-middle Proterozoic (?) Yeoncheon Group. Although the Geonggi Gneiss Complex has been believed to be of Archean-early Proterozoic age, monazites from the sillimanite-garnet gneiss yield a CHIME age of 245±3 Ma. Since one monazite grain from the gneiss contains ca. 1700 Ma core of detrital origin, the sedimentation of the gneiss protolith took place in the post-middle Proterozoic. The two-mica granite, intruding the Gyeonggi Gneiss Complex, yields a CHIME monazite age of 172±5 Ma. The present CHIME geochronological study reveals that metamorphic rocks not only in the Yeonchen Group bur also in some part of the Gyeonggi Gneiss Complex were formed through the ca. 250 Ma regional metamorphism. The late Permian-early Triassic metamorphism and Jurrasic plutonism were more widespread than has been thought in the Korean Peninsula.

INTRODUCTION

The Gyeonggi Massif occupies the central part of the Korean Peninsula, and together with the Yeongnam and Nangrim Massifs, it is one of the major tectonic units where metamorphic rocks widely occur (Fig. 1). Metamorphic rocks in the Gyeonggi Massif are divided into the Gyeonggi Gneiss Complex (Archean-early Proterozoic?) and the Yeoncheon and Seosan Groups (early to middle Proterozoic?). The former consists mainly of high-grade bneiss and schist, while the latter consists dominantly of low-grade schist, phyllite and slate (Na and Kim, 1987).

Three stages of metamorphism have been proposed within the Gyeonggi Massif: (1) Precambrian regional metamorphism of amphibolite facies, (2) post-Precambrian regional metamorphism, and (3) Jurassic thermal event

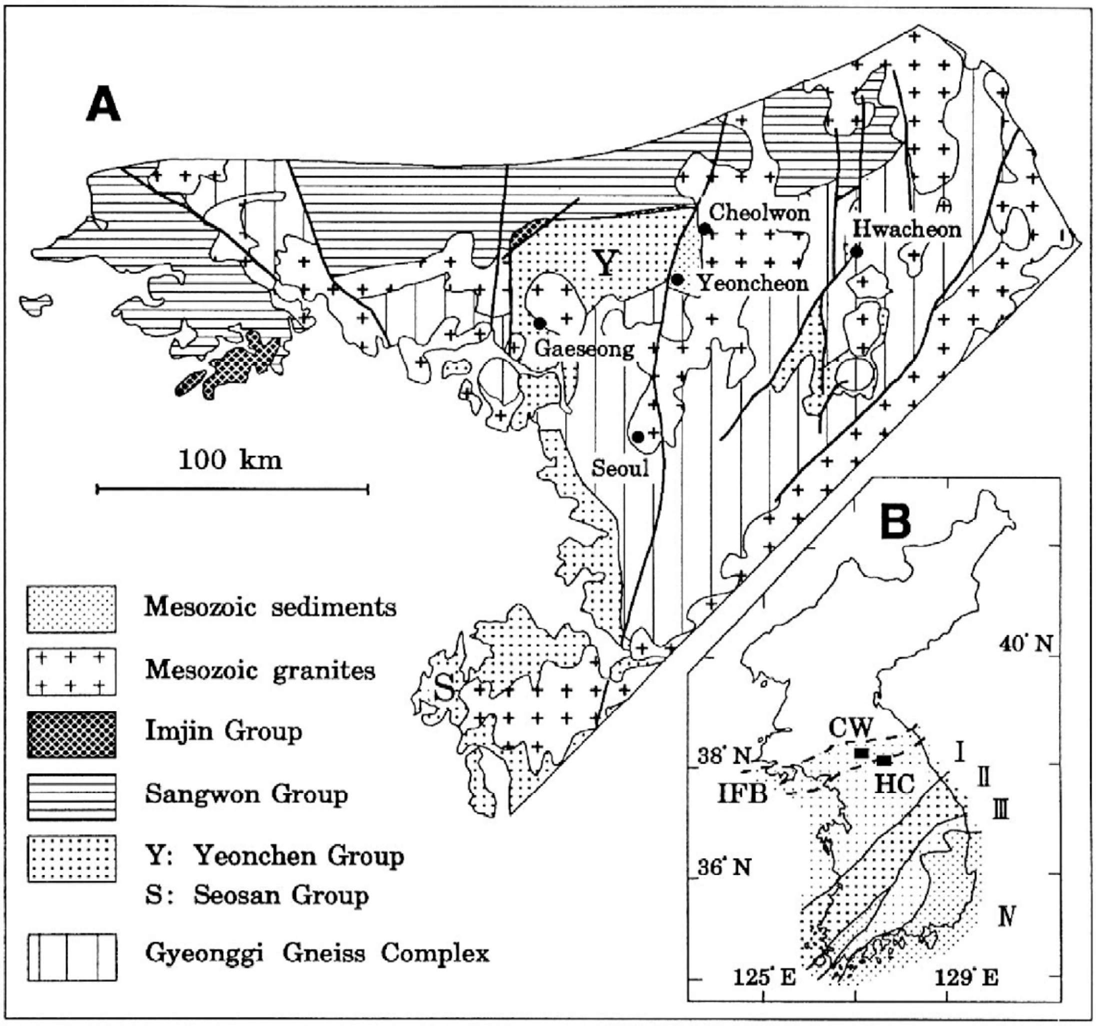

Fig. 1. Geologic framework of the Gyeonggi Massif, and location of the Cheolwon (CW) and Hwacheon (HC) areas. I: Gyeonggi Massif, II: Ogcheon Belt, III: Yeongnam Massif, IV: Gyeongsang Basin and IFB: Imjingang Fold Belt proposed by Ri and Ri (1990) and Cho et al. (1995). The Nangrim Massif distributed in the northern part of the insert map (B) is not shown.

possibly related to the intrusion of the Daebo Granites (Na, 1978). Systematic geochronological studies, however, have not been fully done in this massif, and reported K-Ar, Rb-Sr and Sm-Nd age data are widely scattered from late Proterozoic to middle Jurassic (Na and Lee, 1973; Lee et al., 1974; Na, 1977; Cho et al., 1995; Chwae et al., 1996).

In the northern part of the Gyeonggi Massif, there lies the so-called Imjingang Fold Belt (IFB in Fig. 1). This belt was originally named by North Korean geologists (Ri and Ri, 1990). The western part of the Imjingang Fold Belt is characterized by an EW structural trend, and comprises the Devonian volcano-sedimentary strata of the Imjin Group and some parts of the Gyeonggi Massif including the Yeoncheon Group (Chwae et al., 1996). Recently several authors suggested that the Imjingang Fold Belt rns through the central part of the Kirean Peninsula (Fig. 1), and together with the Ogcheon Fold Belt, it might be an eastward continuation of the Dabie-Sulu Collisional Belt in China (Ri and Ri, 1990; Cluzel et al., 1991; Cluzel, 1992, Liu, 1993; Yin and Nie, 1993; Ernst et al., 1994; Cho et al., 1995). However, northern and southern boundaries as well as westward and eastward continuations of the Imjingang Fold Belt have not been clearly defined yet. Furthermore, no ultra-high pressure indicator like diamond- or coesite-bearing eclogite in the Dabie-Sulu Belt has been known from the imjingang Fold Belt.

To understand the tectonic evolution of the Gyeonggi Massif, we made a preliminary CHIME age determination on monazites from metamorphic rocks of the Yeoncheon Group and the Gyeonggi Gneiss Complex, and a granite intruding the Gyeonggi Gneiss Complex. This is the first CHIME age dating for the Gyeonggi Massif in the Korean Peninsula.

GEOLOGICAL OUTLINE AND SAMPLE DESCRIPTION

Samples were collected from the Yeoncheon Group in the Cheolwon area and the Gyeonggi Gneiss Complex in the Hwacheon area (Fig. 1). These areas have been mapped in 1:50,000 scale under the national basic project of Korea Institute of Geology, Mining and Materials (KIGAM) (Chwae et al., 1996; Park et al., 1997).

Cheolwon area

The geologic map of the Cheolwon area is given in Fig. 2. Metamorphosed strata in this area have been regarded as the Devonian Imjin Group. However, recently Chwae et al. (1996) reported that metamorphosed strata belong to the Yeoncheon Group, and newly devided them into the Misan, Daegwangri and Cheonduksan Formations in ascending order (Fig. 2). The Yeoncheon Group shows a general EW trend with dips toward north, and a reverse shear sense with 340 mineral stretching. Two different types of metamorphic rocks are identified in the Yeoncheon Group; one is low-grade metapsammite, phyllite and crystalline limestone, and the other includes amphibolite-facies pelitic schist of the garnet and kyanite zones of Barrovian type (Cho et al., 1995; Chwae et al., 1996).

One sample of medium-grained kyanite-staurolite-garnet schist (sample CH-10) from the Daegwangri Formation was selected for CHIME age dating (Fig. 2). It consists of quartz, plagioclase, biotite (partly chloritized), muscovite, garnet, staurolite, calcice and kyanite, with accessories of monazite, apatite and rutile. Monazite, tiny, less than 0.05 mm and anhedral, rarely occurs in biotite flakes.

Hwacheon area

The Hwacheon area is about 60 km east of the Cheolwon area (Fig 1). As shown in Fig. 3, this area is underlain by metamorphic rocks and granitoids.

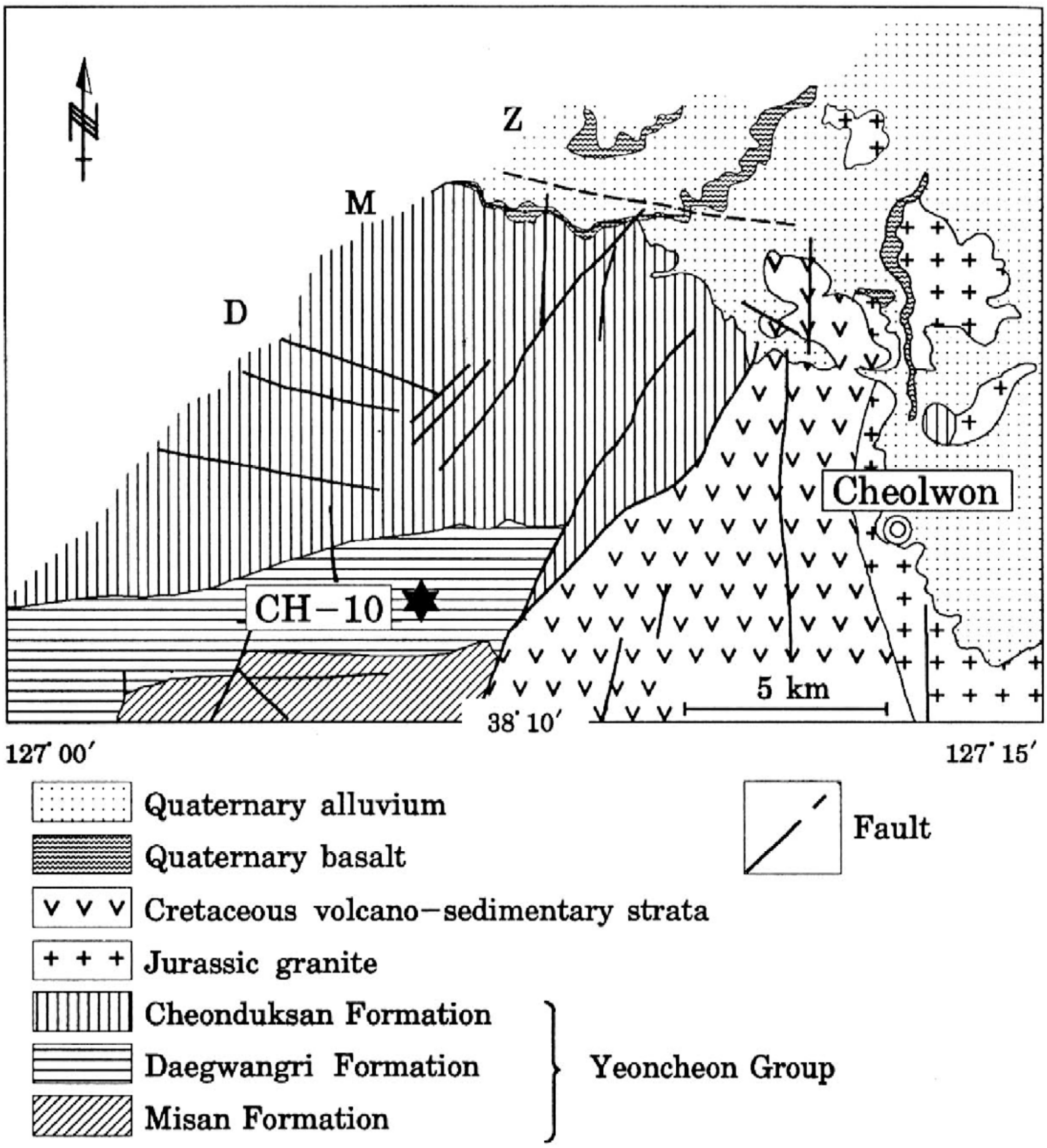

Fig. 2. Geologic map of the Cheolwon area and sample location (simplified and modified from Chwae et al., 1996). The Misan, Daegwangri and Cheonduksan Formations are included in the Middle Proterozoic (?) Yeoncheon Group. DMZ: demilitalized zone.

Several authors suggested that the northern part of the Hwacheon area belongs to the Imjingang Fold Belt (Fig. 1), and has undergone the granulite facies metamorphism (Ri and Ri, 1964; Lee and Cho, 1994; Cho et al., 1995).

Detailed mapping of the Hwacheon area (Park et al., 1997) revealed that amphibolite-facies metasedimentary rocks such as banded gneiss, migmatitic gneiss, biotite gneiss and mica schist are widely exposed, with subordinate garnet-bearing granite gneiss and amphibolite. The metasedimentary rocks of the Gyeonggi Gneiss Complex show well-developed gneissosity or schistosity. These planar structures show major trends of NE and NS. The EW

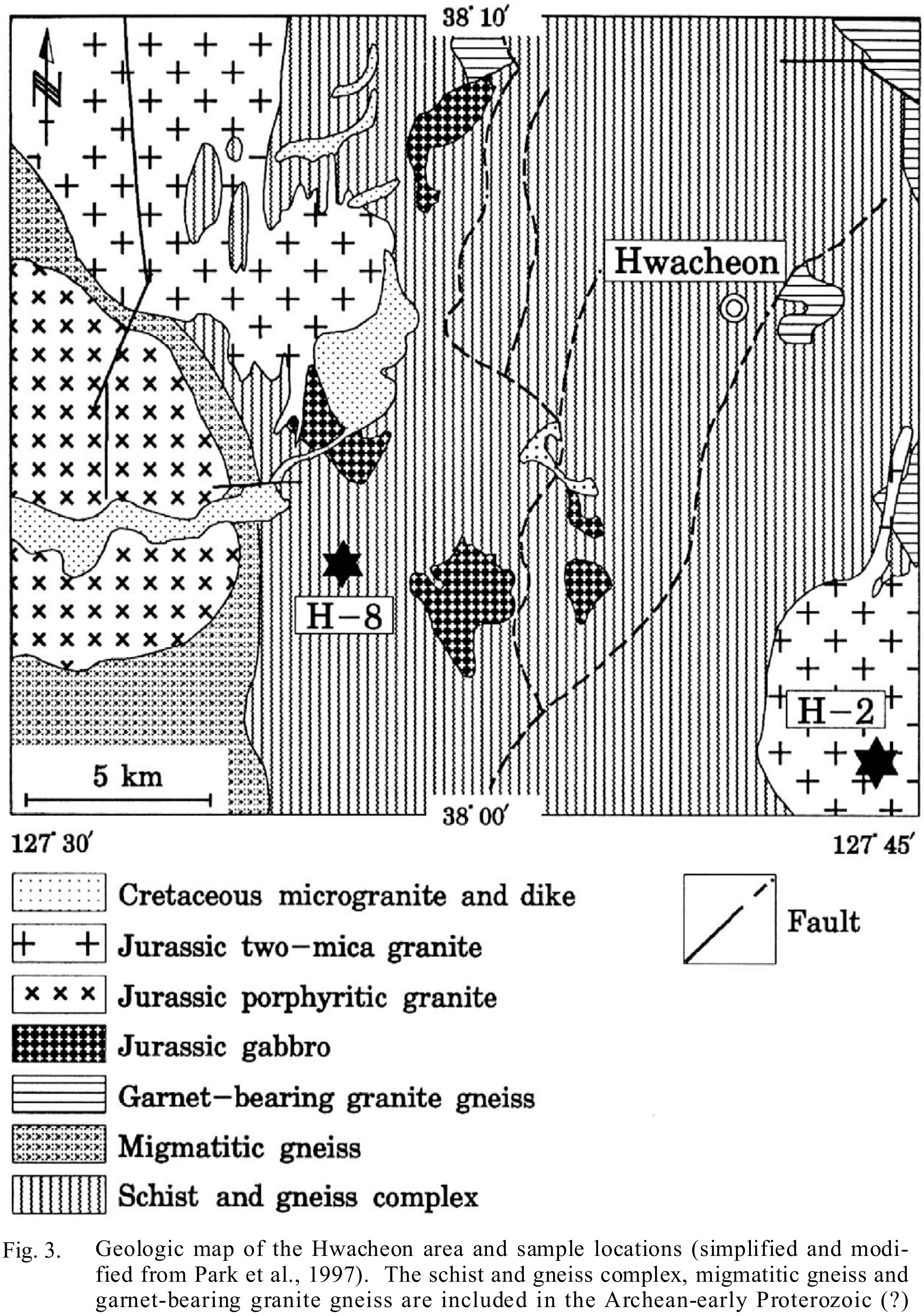

Fig. 3. Geologic map of the Hwacheon area and sample locations (simplified and modified from Park et al., 1997). The schist and gneiss complex, migmatitic gneiss and garnet-bearing granite gneiss are included in the Archean-early Proterozoic (?) Gyeonggi Gneiss Complex.

structural trend, dominant in the Cheolwon area, does not continue to the Hwacheon area.

Two samples were chosen for CHIME age dating (Fig. 3). They are sillimanite-garnet gneiss of the Gyeonggi Gneiss Complex and two-mica granite intruding the Gneiss Complex. The sillimanite-garnet gneiss (sample H-8) is medium-grained and consists of quartz, plagioclase, orthoclase, sillimanite, garnet, biotite and muscovite, with accessories of monazite, zircon (round), apatite and rutile. Small monazite grains are commonly found in biotite flakes. They are mostly 0.07-0.1 mm and subhedral, but larger (up to 0.2 mm) anhedral grains also occur rarely.

The two-mica granite (sample H-2) is massive and medium-grained, consisting mainly of quartz, plagioclase, perthitic microcline, biotite, muscovite and garnet. Accessory minerals include monazite and zircon. Hydrothermal or deuteric alteration of the granite is indicated by ubiquitous occurrence of sericite in plagioclase and chloritized biotite. Monazite grains, 0.03-0.1 mm, are subhedral or euhedral.

SAMPLE PREPARATION AND ANALYSIS

Monazites in polished thin sections and/or mounted on glass slides with petropoxy were analyzed by using the JEOL JCXA-733 electron microprobe. Since details on procedures of sample preparation, microprobe analysis and CHIME age calculation were described elsewhere (Suzuki and Adachi, 1991a,b, 1994; Suzuki et al., 1991, 1994), we do not repeat them here. The ThO_2, UO_2 and PbO analyses of monazites, apparent ages and calculated ThO_2* concentrations are listed in Table 1.

RESULTS

Kyanite-staurolite-garnet schist (sample CH-10) from the Daegwangri Formation of the Yeoncheon Group

A total of 29 spots on 6 monazite grains were analyzed in polished thin sections. One monazite grain (M03) is eztraordinarily rich in ThO_2 (23.0-28.2%) and UO_2 (1.54-2.14%), and is highly metamict. Spot M01-6, containing 19.8% ThO2 and 1.31% UO2, is also metamict. Except these data (cross in Fig. 4), the rest 24 data (circle in Fig. 4) show 3.50-12.5% if ThO_2, 0.10-0.65% of UO_2 and 0.044-0.140% of PbO. They are regressed by an isochron of 255±8 Ma (MSWD=0.10) with an intercept value of -0.0011±0.0025 (errors quoted in this paper for ages and intercept values are of 2σ).

Sillimanite-garnet gneiss (sample H-8) from the Gyeonggi Gneiss Complex

A total of 172 spots on 21 monazite grains were analyzed. Apparent ages of the most grains concentrate between 235 Ma and 258 Ma, and 118 data points (circle in Fig. 5) yield an isochron age of 245±3 Ma (MSWD=0.05) with an intercept value of -0.0001±0.0011 in the PbO vs. ThO_2* plot. The core part of

Table 1. Electron microprobe analyses of ThO_2, UO_2 and PbO of monazite grains from kyanite-staurolite-garnet schist of the Yeoncheon Group and sillimanite-garnet gneiss and two-mica granite in the Gyeonggi Gneiss Complex, Korea.

Spot#	ThO_2 (wt.%)	UO_2 (wt.%)	PbO (wt.%)	Age (Ma)	ThO_2* (wt.%)
	Kyanite-staurolite-garnet schist (Sample CH-10)				
M01-01	3.50	0.210	0.0440	249	4.18
M01-02	4.23	0.451	0.0593	246	5.69
M01-03	5.92	0.144	0.0716	265	6.39
M01-04	8.26	0.160	0.0946	255	8.78
M01-05	8.99	0.253	0.103	247	9.81
M01-06	9.75	0.179	0.113	259	10.3
M02-01	10.3	0.184	0.114	246	10.9
M02-02	12.5	0.125	0.140	256	12.9
M02-03	6.69	0.096	0.0715	241	7.01
M02-04	6.87	0.132	0.0778	252	7.30
M03-01 m	24.7	1.54	0.200	160	29.6
M03-02 m	27.3	2.14	0.208	144	34.1
M03-03 m	22.9	1.98	0.117	95	29.3
M03-04 m	28.1	2.09	0.137	93	34.8
M04-01	4.22	0.232	0.0526	250	4.97
M04-02	7.09	0.328	0.0866	251	8.16
M05-01	6.29	0.239	0.0725	243	7.06
M05-02	5.26	0.216	0.0632	251	5.96
M05-03	5.01	0.144	0.0578	249	5.47
M05-04	4.43	0.255	0.0572	257	5.26
M05-05	4.82	0.469	0.0676	252	6.34
M05-06	7.75	0.451	0.0951	244	9.21
M05-07	3.93	0.646	0.0680	267	6.02
M05-08	4.24	0.288	0.0534	244	5.17
M06-01 m	19.8	1.311	0.206	202	24.0
M06-02	3.88	0.365	0.0530	247	5.06
M06-03	4.41	0.435	0.0611	248	5.82
M06-04	8.95	0.247	0.105	254	9.75
M06-05	8.46	0.266	0.100	254	9.32

ThO_2*: sum of the measured ThO2 and ThO_2 equivalent of the measured UO_2

Note;

m: metamict part of monazite grain
c: core part of monazite grain
r: rim part of monazite grain
s: sillimanite-containing monazite grain
t: tiny monasite grain

Spot#	ThO_2 (wt.%)	UO_2 (wt.%)	PbO (wt.%)	Age (Ma)	ThO_2* (wt.%)
	Sillimanite-garnet gneiss (Sample H-8)				
M01-01	5.47	0.304	0.0662	242	6.46
M01-02	5.71	0.297	0.0663	235	6.68
M01-03	5.50	0.321	0.0688	249	6.53
M01-04	5.15	0.376	0.0663	246	6.37
M01-05	6.60	0.331	0.0778	240	7.67
M01-06	3.76	0.353	0.0502	242	4.90
M01-07	5.04	0.406	0.0658	244	6.36
M01-08	6.00	0.415	0.0760	244	7.35
M01-09	4.58	0.402	0.0643	258	5.89
M01-10	6.10	0.376	0.0759	245	7.32
M02-01	5.05	0.389	0.0665	249	6.31
M02-02	5.97	0.340	0.0729	244	7.07
M02-03	6.12	0.373	0.0760	245	7.33
M02-04	5.97	0.363	0.0726	240	7.15
M02-05	5.76	0.305	0.0701	246	6.75
M02-06	5.52	0.348	0.0689	245	6.65
M02-07	5.78	0.336	0.0716	246	6.86
M02-08	5.08	0.289	0.0618	243	6.02
M02-09	4.86	0.372	0.0632	246	6.06
M02-10	5.46	0.393	0.0695	244	6.74
M02-11	3.77	0.389	0.0521	245	5.03
M02-12	5.84	0.294	0.0701	244	6.79
M03-01 s	5.18	0.136	0.0441	186	5.62
M03-02 s	5.37	0.176	0.0459	183	5.93
M03-03 s	4.34	0.462	0.0588	238	5.84
M03-04 s	5.10	0.150	0.0478	202	5.58
M03-05 s	5.73	0.195	0.0495	184	6.36
M04-01	8.73	0.354	0.101	243	9.87
M04-02	10.3	0.398	0.120	244	11.6
M04-03	6.81	0.417	0.0845	245	8.16
M04-04	10.1	0.465	0.117	238	11.6
M04-05	11.7	0.518	0.139	246	13.4
M04-06	6.60	0.272	0.0770	243	7.48
M05-01	5.87	0.320	0.0729	250	6.90
M05-02	7.93	0.445	0.0958	241	9.38
M05-03	5.64	0.458	0.0726	241	7.12
M05-04	6.25	0.384	0.0782	246	7.50
M05-05	6.03	0.336	0.0760	252	7.12
M05-06	6.10	0.482	0.0782	241	7.67
M05-07	5.43	0.510	0.0720	240	7.08
M06-01	3.69	0.472	0.0531	240	5.22

Table 1. (continued).

Spot#	ThO_2 (wt.%)	UO_2 (wt.%)	PbO (wt.%)	Age (Ma)	ThO_2* (wt.%)
M06-02	3.12	0.491	0.0487	244	4.71
M06-03	8.87	0.490	0.108	244	10.5
M06-04	6.61	0.403	0.0802	239	7.91
M07-01	6.93	0.484	0.0875	243	8.50
M07-02	11.2	0.404	0.129	242	12.5
M07-03	9.63	0.389	0.114	247	10.9
M08-01d	5.62	0.382	0.511	1661	7.03
M08-02d	5.56	0.392	0.518	1690	7.00
M08-03d	5.54	0.415	0.520	1682	7.06
M08-04d	5.65	0.399	0.531	1701	7.12
M08-05 d	5.61	0.395	0.508	1644	7.06
M08-06d	5.57	0.407	0.523	1687	7.07
M08-07d	5.42	0.365	0.513	1730	6.77
M08-08d	5.33	0.366	0.508	1733	6.68
M08-09d	5.40	0.421	0.508	1670	6.95
M08-10d	5.49	0.406	0.500	1637	6.98
M08-11r	6.47	0.294	0.0626	199	7.42
M08-12	6.65	0.270	0.0753	237	7.52
M08-13	5.57	0.267	0.0633	232	6.44
M08-14	5.42	0.244	0.0644	245	6.21
M08-15	5.71	0.248	0.0591	215	6.51
M08-16d	5.80	0.413	0.551	1717	7.32
M08-17d	5.74	0.419	0.497	1567	7.26
M08-18	4.61	0.258	0.0560	243	5.44
M08-19	4.36	0.282	0.0569	255	5.28
M08-20d	5.60	0.348	0.143	497	6.75
M08-21	6.34	0.331	0.0698	223	7.41
M08-22d	5.91	0.344	0.533	1697	7.17
M08-23d	5.54	0.328	0.510	1723	6.75
M08-24d	7.12	0.379	0.197	552	8.38
M08-25d	5.43	0.391	0.509	1691	6.87
M08-26d	5.65	0.373	0.529	1718	7.03
M09-01	5.92	0.579	0.0842	255	7.79
M09-02	5.99	0.607	0.0841	250	7.95
M09-03	5.51	0.558	0.0750	242	7.32
M10-01	5.56	0.316	0.0699	251	6.59
M10-02 r	5.37	0.327	0.0516	190	6.43
M10-03 r	5.46	0.313	0.0584	213	6.47
M10-04	5.09	0.317	0.0616	238	6.12
M10-05	5.44	0.312	0.0663	243	6.45
M11-02	5.55	0.310	0.0695	250	6.56
M11-02	6.22	0.441	0.0799	247	7.64
M11-03	6.87	0.379	0.0839	245	8.10
M11-04	6.59	0.314	0.0791	246	7.61

Spot#	ThO_2 (wt.%)	UO_2 (wt.%)	PbO (wt.%)	Age (Ma)	ThO_2* (wt.%)
M11-05	9.35	0.457	0.113	245	10.8
M12-01t	5.19	0.182	0.0502	205	5.78
M12-02t	5.88	0.173	0.0495	182	6.44
M12-03t	6.13	0.168	0.0564	200	6.67
M12-04t	6.11	0.173	0.0621	220	6.67
M13-01	6.46	0.360	0.0786	244	7.62
M13-02	7.20	0.473	0.0890	241	8.74
M13-03r	5.72	0.243	0.0492	179	6.51
M13-04	5.76	0.233	0.0673	244	6.51
M14-01	11.1	0.373	0.127	245	12.3
M14-02	11.2	0.348	0.129	246	12.3
M14-03	8.96	0.528	0.110	244	10.7
M14-04	10.1	0.377	0.119	249	11.3
M14-05	13.2	0.324	0.149	247	14.3
M15-01r	5.68	0.151	0.0500	192	6.17
M15-02	5.57	0.157	0.0646	251	6.08
M15-03	5.90	0.165	0.0630	231	6.43
M15-04	5.62	0.150	0.0624	242	6.10
M16-01r	5.33	0.397	0.0646	231	6.61
M16-02	5.26	0.362	0.0655	241	6.44
M16-03r	5.67	0.363	0.0628	217	6.84
M16-04r	6.64	0.450	0.0825	241	8.10
M16-05	6.21	0.501	0.0834	252	7.83
M16-06r	6.59	0.461	0.0797	233	8.09
M16-07r	4.99	0.422	0.0622	231	6.35
M16-08	5.71	0.427	0.0739	246	7.09
M16-09	5.51	0.383	0.0696	244	6.75
M16-10	6.04	0.342	0.0745	246	7.15
M16-11	5.51	0.355	0.0714	253	6.66
M16-12	5.30	0.343	0.0644	237	6.41
M16-13r	4.38	0.388	0.0564	236	5.64
M16-14r	5.93	0.397	0.0699	229	7.21
M16-15	6.31	0.400	0.0830	258	7.60
M16-16	5.86	0.353	0.0730	246	7.00
M16-17	5.66	0.362	0.0712	246	6.84
M16-18	5.60	0.341	0.0698	246	6.71
M16-19	5.31	0.324	0.0678	252	6.36
M16-20	5.62	0.353	0.0695	243	6.76
M16-21	4.42	0.276	0.0573	255	5.32
M16-22r	5.99	0.359	0.0714	236	7.15
M16-23r	5.61	0.294	0.0590	213	6.56
M16-24	5.39	0.312	0.0650	240	6.40
M16-25	5.73	0.269	0.0681	244	6.60
M16-26	5.44	0.290	0.0671	248	6.39

Table 1. (continued).

Spot#	ThO_2 (wt.%)	UO_2 (wt.%)	PbO (wt.%)	Age (Ma)	ThO_2* (wt.%)
M16-27	4.91	0.275	0.0600	245	5.80
M16-28	5.86	0.340	0.0709	241	6.96
M16-29r	6.34	0.308	0.0695	224	7.33
M16-30r	5.24	0.335	0.0601	225	6.32
M16-31	6.18	0.460	0.0778	240	7.67
M16-32	5.00	0.329	0.0630	245	6.07
M16-33	5.88	0.332	0.0725	246	6.95
M16-34	5.56	0.323	0.0683	244	6.61
M16-35	5.57	0.264	0.0669	246	6.42
M16-36	6.06	0.289	0.0713	241	7.00
M16-37	6.06	0.307	0.0716	240	7.05
M16-38r	5.95	0.302	0.0697	238	6.93
M17-01	5.17	0.271	0.0620	242	6.05
M17-02	5.43	0.292	0.0648	240	6.38
M17-03	5.35	0.306	0.0661	246	6.34
M17-04	5.65	0.252	0.0642	235	6.46
M17-05	5.34	0.276	0.0639	242	6.23
M18-01	4.69	0.266	0.0602	256	5.55
M18-02	5.37	0.285	0.0642	241	6.29
M18-03	4.71	0.270	0.0596	252	5.59
M18-04	4.65	0.384	0.0585	235	5.89
M18-05	5.92	0.373	0.0749	248	7.13
M19-01r	4.89	0.266	0.0497	205	5.74
M19-02	5.11	0.279	0.0616	242	6.02
M19-03	5.12	0.289	0.0606	236	6.06
M19-04r	3.92	0.539	0.0519	217	5.66
M19-05	5.31	0.329	0.0659	244	6.38
M20-01	7.09	0.305	0.0825	241	8.08
M20-02	5.47	0.330	0.0682	246	6.54
M20-03	5.29	0.289	0.0659	250	6.22
M20-04	5.68	0.336	0.0747	261	6.77
M20-05	4.98	0.247	0.0574	235	5.78
M20-06	4.98	0.250	0.0588	240	5.79
M20-07	5.66	0.275	0.0696	251	6.55
M20-08	4.55	0.269	0.0540	235	5.42
M21-01	5.19	0.295	0.0626	241	6.15
M21-02	5.11	0.304	0.0645	250	6.09
M21-03	5.21	0.284	0.0633	244	6.13
M21-04	5.13	0.294	0.0642	250	6.08
M21-05	5.01	0.274	0.0633	253	5.90
M21-06	5.46	0.305	0.0672	246	6.45
M21-07	4.83	0.256	0.0580	242	5.66
M21-08r	4.96	0.247	0.0504	207	5.76

Spot#	ThO_2 (wt.%)	UO_2 (wt.%)	PbO (wt.%)	Age (Ma)	ThO_2* (wt.%)
	Two-mica granite (Sample H-2)				
M01-01	9.89	0.275	0.0780	171	10.8
M01-02	10.6	0.206	0.0883	185	11.3
M01-03	10.5	0.198	0.0806	171	11.2
M01-04c	5.99	0.146	0.0529	194	6.46
M01-05	10.2	0.187	0.0848	186	10.8
M01-06	8.51	0.202	0.0669	173	9.16
M01-07c	5.40	0.182	0.0539	213	5.99
M01-08	10.4	0.186	0.0802	172	11.0
M01-09	5.58	0.137	0.0415	163	6.03
M02-01c	5.26	0.132	0.0484	201	5.69
M02-02	4.73	0.121	0.0380	175	5.12
M02-03	13.5	0.214	0.107	178	14.2
M02-04	14.0	0.248	0.112	179	14.8
M02-05	12.8	0.198	0.101	178	13.4
M02-06	13.1	0.200	0.0967	167	13.7
M02-07	13.9	0.243	0.100	161	14.7
M02-08	17.8	0.373	0.141	175	19.0
M02-09	13.2	0.218	0.100	170	13.9
M02-10	9.31	0.187	0.0776	185	9.910
M02-11	12.3	0.209	0.0938	171	12.9
M02-12c	8.99	0.151	0.0818	204	9.48
M02-13r	6.13	0.309	0.0419	139	7.12
M02-14	8.59	0.224	0.0629	160	9.31
M02-15c	8.83	0.161	0.0791	200	9.35
M02-16c	5.65	0.550	0.0639	203	7.43
M03-01	9.53	0.084	0.0762	184	9.80
M03-02	9.86	0.104	0.0760	176	10.2
M03-03	10.2	0.150	0.0754	168	10.6
M03-04	8.99	0.110	0.0641	162	9.34
M03-05	9.86	0.109	0.0803	186	10.2
M03-06	6.87	0.055	0.0508	170	7.05
M03-07	6.91	0.033	0.0525	177	7.03
M03-08c	10.38	0.117	0.0935	205	10.8
M03-09c	10.2	0.097	0.0884	199	10.5
M03-10	10.0	0.114	0.0809	185	10.4
M03-11	10.0	0.100	0.0806	184	10.4
M03-12	9.63	0.097	0.0695	165	9.94
M03-13c	10.3	0.099	0.0878	195	10.6
M03-14	10.4	0.117	0.0783	173	10.7
M03-16	10.1	0.095	0.0767	174	10.4
M04-01	8.53	0.224	0.0716	183	9.25
M04-02	4.03	0.083	0.0326	180	4.29

Table 1. (continued).

Spot#	ThO_2 (wt.%)	UO_2 (wt.%)	PbO (wt.%)	Age (Ma)	ThO_2* (wt.%)
M04-03	4.71	0.134	0.0415	191	5.15
M04-04c	7.11	0.043	0.0605	197	7.25
M04-05	8.54	0.048	0.0661	180	8.69
M05-01	5.78	0.222	0.0472	172	6.49
M05-02r	5.81	0.240	0.0268	96	6.58
M05-03	7.83	0.379	0.0609	159	9.06
M05-04	6.30	0.133	0.0523	184	6.73
M05-05r	6.82	0.197	0.0236	75	7.45
M05-06r	6.14	0.340	0.0353	116	7.23
M05-07	5.04	0.189	0.0454	190	5.65
M05-08	6.13	0.260	0.0569	193	6.97
M05-09r	6.03	0.361	0.0224	74	7.19
M05-10r	6.56	0.150	0.0386	130	7.04
M05-11	6.25	0.110	0.0453	162	6.60
M05-12	6.24	0.166	0.0453	158	6.77
M05-13	5.78	0.131	0.0425	162	6.20
M05-14r	5.29	0.125	0.0316	131	5.69
M05-15	6.61	0.179	0.0481	158	7.18
M05-16r	6.40	0.173	0.0435	148	6.96
M05-17	4.95	0.081	0.0409	186	5.21
M05-18c	3.06	0.107	0.0332	231	3.40
M05-19r	4.56	0.105	0.0249	120	4.90
M05-20	3.88	0.102	0.0326	183	4.20
M05-21	4.14	0.086	0.0288	154	4.41
M05-22r	5.07	0.131	0.0340	147	5.49
M05-23	6.18	0.142	0.0447	159	6.64
M05-24r	5.87	0.088	0.0382	147	6.15
M05-25	3.96	0.036	0.0272	158	4.08
M05-26c	3.55	0.040	0.0378	243	3.68
M05-27r	6.45	0.145	0.0437	150	6.91
M05-28r	6.07	0.152	0.0382	138	6.56
M05-29	5.95	0.139	0.0459	170	6.40
M05-30r	5.08	0.121	0.0356	154	5.47
M05-31r	3.80	0.108	0.0252	144	4.14
M05-32	4.01	0.097	0.0327	179	4.32
M05-33	3.87	0.083	0.0285	163	4.14
M05-34	4.73	0.069	0.0391	187	4.94
M05-35	5.82	0.192	0.0429	158	6.44
M05-36	5.55	0.157	0.0433	169	6.06
M05-37r	5.26	0.144	0.0359	148	5.72
M05-38	4.45	0.136	0.0451	218	4.89
M05-39c	6.64	0.342	0.0662	202	7.74
M05-40c	3.88	0.100	0.0365	205	4.20
M05-41	3.69	0.080	0.0304	182	3.95
M05-42r	2.42	0.179	0.0177	140	3.00
M05-43	3.71	0.094	0.0294	173	4.01
M05-44c	3.43	0.116	0.0313	194	3.81
M04-45	3.39	0.112	0.0248	156	3.75
M05-46	3.16	0.070	0.0238	167	3.38
M05-47	3.59	0.091	0.0281	171	3.88
M05-48r	6.24	0.060	0.0403	148	6.43
M05-49	4.96	0.119	0.0349	155	5.34
M05-50r	4.25	0.115	0.0258	132	4.62
M05-51	3.58	0.120	0.0295	176	3.97
M05-52r	1.96	0.314	0.0167	133	2.97
M05-53	3.20	0.122	0.0270	177	3.60
M05-54r	2.64	0.211	0.0185	132	3.32
M05-55r	2.76	0.124	0.0198	148	3.16
M05-56	3.24	0.185	0.0254	157	3.84
M05-57	3.37	0.103	0.0252	161	3.71
M05-58	3.88	0.104	0.0301	169	4.21
M05-59c	3.73	0.105	0.0344	200	4.07
M05-60	2.84	0.106	0.0257	191	3.18
M05-61r	3.60	0.250	0.0189	101	4.40
M05-62r	2.89	0.199	0.0221	148	3.53
M05-63	2.19	0.154	0.0209	184	2.69
M05-64	1.72	0.191	0.0193	196	2.33
M05-65	1.79	0.306	0.0227	193	2.78
M05-66	2.71	0.174	0.0231	167	3.28
M05-67c	3.58	0.176	0.0404	230	4.14
M05-68r	3.40	0.128	0.0198	123	3.81
M05-69c	5.19	0.055	0.0468	206	5.37
M05-70	3.83	0.118	0.0293	165	4.21
M05-71	3.22	0.116	0.0288	190	3.59
M05-72c	3.28	0.112	0.0351	228	3.64
M05-73	3.98	0.047	0.0328	188	4.13
M05-74	3.07	0.002	0.0220	169	3.07
M05-75	4.34	0.065	0.0352	183	4.55
M05-76c	3.79	0.096	0.0452	261	4.10
M05-77	4.56	0.122	0.0369	176	4.96
M05-78c	4.81	0.109	0.0456	209	5.16
M05-79	3.53	0.071	0.0294	185	3.76
M05-80r	4.98	0.109	0.0286	127	5.33
M05-81	3.90	0.328	0.0332	158	4.96
M05-82	3.30	0.265	0.0305	174	4.16
M05-83	6.60	0.184	0.0568	187	7.19

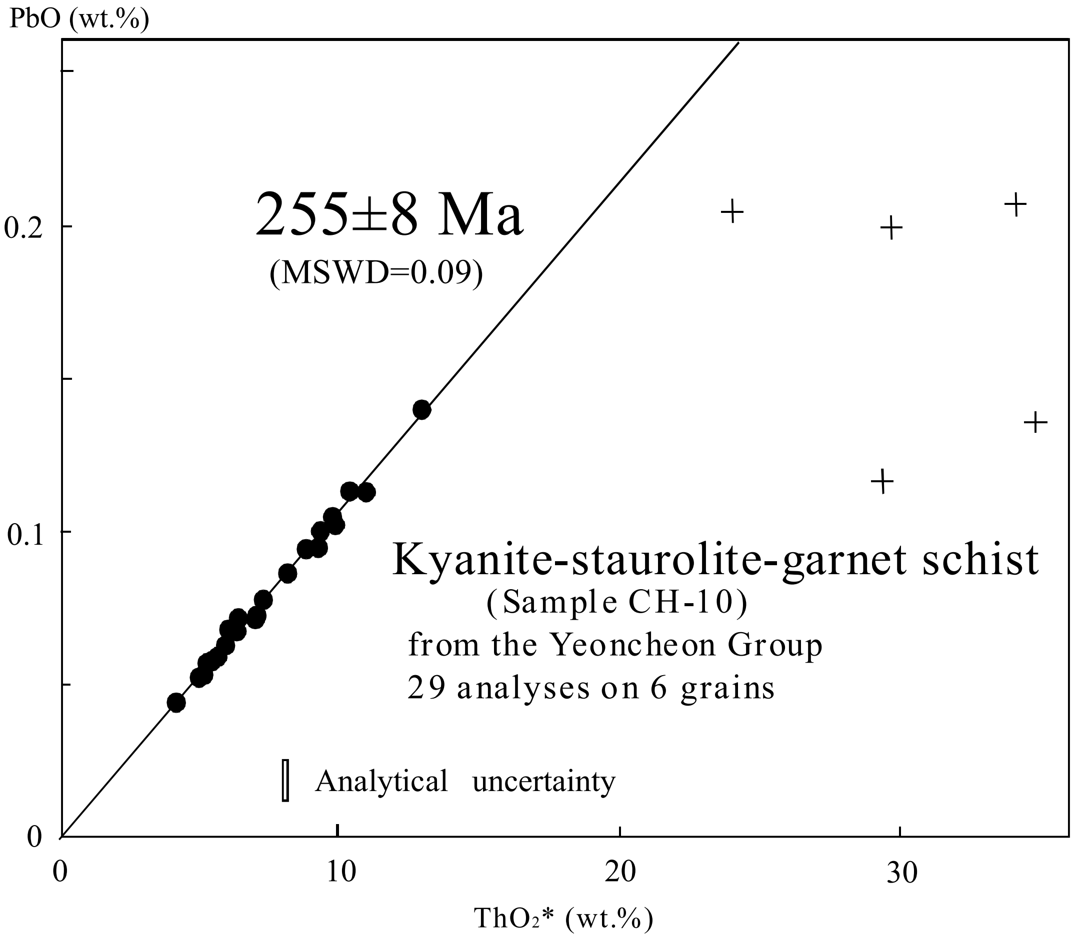

Fig. 4. Plots of PbO vs. ThO_2* of monazite grains from the kyanite-staurolite-garnet schist (sample CH-10) of the Yeoncheon Group. Circles represent data points for transparent portions, and crosses do data points for metamict portions. Error box in the figure represents 2σ analytical uncertainty, and error quoted for age is of 2σ.

M8 grain (square in Fig. 5) is much older than others, concentrating around the 1700 Ma reference isochron. The core also differs in composition (ThO_2/UO_2=12-17) from the ca. 245 Ma rim (ThO_2/UO_2=15-24). The ca. 1700 Ma core, formed under different chemical environments from the ca. 245 Ma rim, appears to be detrital. One monazite grain (M03) contains sillimanite (fibrolite) in its rim portion, indicating an overgrowth after the formation of sillimanite. The core of M03 grain shows 238 Ma apparent ages, while the sillimanite-containing rim gives 183-186 Ma apparent ages. Similar young ages (cross in Fig. 5) are also recognized from a timy grain (M12) and rims of some large grains (M13 and M15). The age zoning of monazite suggests that the sillimanite-garnet gneiss underwent an intensive thermal event during Jurassic time after the ca. 245 Ma high-grade metamorphism.

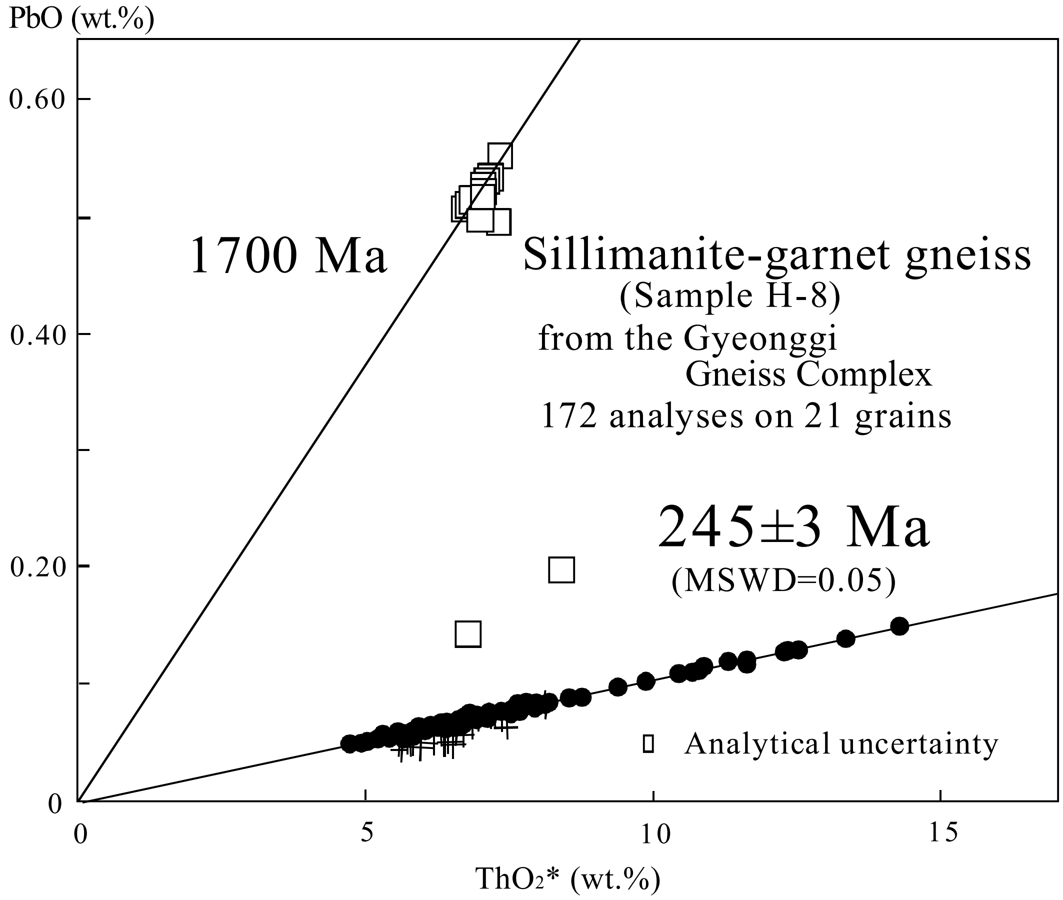

Fig. 5. Plots of PbO vs. ThO_2* of monazite grains from the sillimanite-garnet gneiss in the Gyeonggi Gneiss Complex (sample H-8). Circles represent data points used for age calculation. Data points for the core of zoned M08 grain are shown by squares, and those for sillimanite-containing M03 grain, tiny M12 grain and rim portions of unzoned grains are shown by crosses. Explanation for errors is the same as Fig. 3.

Two-mica granite (sample H-2) from the Gyeonggi Gneiss Complex

A total of 128 spots on 5 monazite grains were analyzed. Some spots on the cores of individual grains (square in Fig. 6) show apparent ages of 190-261 Ma, and those on grain edges and rough-surface parts (cross in Fig. 6) give younger apparent ages of 74-154 Ma. Except these, the rest 80 data (circle in Fig. 6), showing 1.72-17.83% ThO_2, 0.00-0.38% UO_2 and 0.019-0.141% PbO, yield an isochron of 172±5 Ma (MSWD=0.45) with an intercept value -0.0003±0.0012. The core age corresponds to the age for the sillimanite-garnet gneiss of the Gyeonggi Gneiss Complez in which the two-mica granite intruded. The older cores are xenocrysts derived from surrounding gneisses. They might survive from entire loss of Pb during the granite consolidation, since the closure temperature of Pb diffusion in monazite (650-700℃, Suzuki et al., 1994) is close to the solidus temperature of hydrous granitic magma at moderate pressures (Stern et al., 1975).

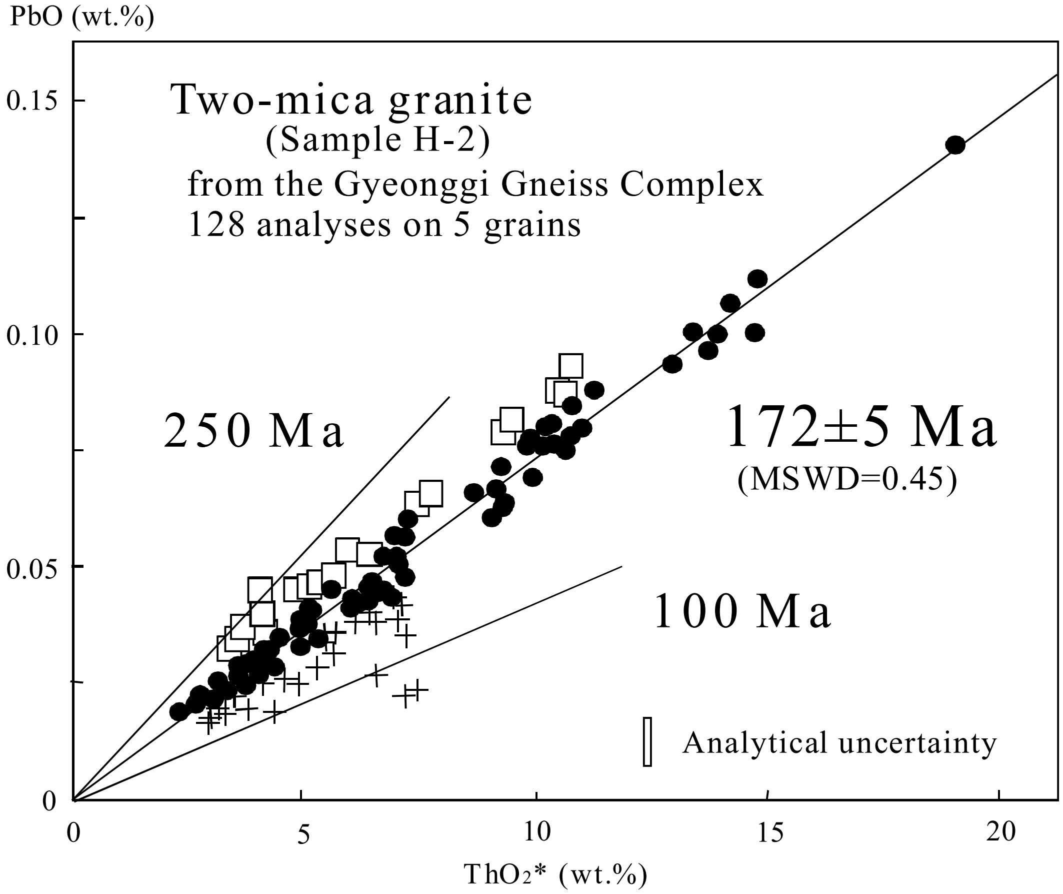

Fig. 6. Plots of PbO vs. ThO_2* of monazite grains from the two-mica granite (sample H-2) in the Gyeonggi Gneiss Complex. Circles represent data points used for age calculation. Data points for core and rim portions of individual grains are shown by squares and crosses, respectively. Explanation for errors is the same as Fig. 3.

K-Ar muscovite age of this two-mica granite is 151±4 Ma (Park et al., 1997). The blocking temperature of muscovite (350±50°C, Dodson and McClelland-Brown, 1985) is lower than that of monazite (650-700°C, Suzuki et al., 1994). Since most of the Jurassic Daebo Granites cooled slowly at middle crust level (Cho and Kwon, 1994) after the consolidation, the CHIME monazite and K-Ar muscovite ages are reasonably regarded as the time of emplacement and subsequent cooling of the two-mica granite.

DISCUSSION

Monazite begins to form as metamorphic mineral at the lower amphibolite-facies condition (Smith and Barreiro, 1990). Thus, the CHIME monazite age of 255±8 Ma for the kyanite-staurolite-garnet schist can be regarded as the time of the regional metamorphism for the early-middle Proterozoic Yeoncheon Group in the so-called Imjingang Fold Belt. The metamorphic age for the

Yeoncheon Group was also dated through the Sm-Nd and Rb-Sr minneral isochron methods (Cho et al., 1995). The Sm-Nd and Rb-Sr garnet-plagioclase-whole rock isochron ages of amphibolite from the Misan Formation are 231±30 Ma and 224±24 Ma, respectively. Although the ages are overlapped within error limits, the CHIME monazite age appears to be significantly older than the isotopic ages. Presumably, the CHIME monazite age represents the time for the first attainment of the lower amphibolite facies, and the Sm-Nd and Rb-Sr ages date the time of cooling related to uplift.

The sillimanite-garnet gneiss from the Gyeonggi Gneiss Complex gives CHIME monazite age of 245±3 Ma. As stated earlier, this gneiss sample contains monazite with ca. 1700 Ma core of detrital origin. Therefore, the sedimentation age of the gneiss protolith is post-middle Proterozoic. This clearly demonstrates that all of the Gyeonggi Gneiss Complex is not the Archean-early Proterozoic complex so far believed (Na and Kin, 1987; Ri and Ri, 1994; Chwae, et al., 1995). The post-middle Proterozoic sediment underwent the late Permian-early Triassic amphibolite-facies metamorphism and the Jurassic thermal event.

Despite the different geologic province and tectonic setting (Figs. 1, 2 and 3), CHIME monazite ages for the Yeoncheon Group and the Gteonggi Gneiss Complex are nearly identical. This suggests that the late Permian-early Triassic regional metamorphism occurred not only in the Imjingan Fold Belt but also in some parts of the Gyeonggi Gneiss Complex. The late-Permian-early Triassic regional metamorphism is also recognized from the central part of the Ogcheon Fold Belt in the Korean Peninsula (Adachi et al., 1996). Outside the Korean Peninsula, the late Permian-early Triassic regional metamorphism occurred in the Hida Terrane, Southwest Japan (Suzuki and Adachi, 1994), the Qinling-Dabie-Sulu Collisional Belt, China (Lie, 1993) and so on. Although many hypotheses on the tectonic correlation of China-Korea-Japan-Russia have been proposed (Adachi et al., 1996; Suzuki and Adachi, 1994; Cluzel, 1992; Ernst et al., 1994, Liu, 1993; Yin and Nie, 1993), details in terms of tectonics are still unclear.

It is noteworthy that the metamorphic rocks of the Yeoncheon Group and the Gyeonggi Gneiss Complex are particularly comparable in mineral assemblage as well as in age with the Unazuki Schist of the Barronvian type and the Hida Gneiss of the Buchan type in the Hida terrane of central Japan, respectively. The Yeoncheon Group and the Gyeonggi Gneiss Complex were extensively intruded by the Jurassic Daebo Granites including the 172±5 Ma two-mica granite, and the Unazuki Schist and the Hida Gneiss in central Japan were intruded by the ca. 175-190 Ma (Shibata and Nozawa, 1984; Khan et al., 1995) Funatsu Granite. The overall similarlity in metamorphic age, mineral assemblage and plutonic age shows that both the Gyeonggi Massif in the Kirean Peninsula and the Hida terrane in central Japan once shared a common geologic province.

CONCLUDING REMARKS

On the basis of the preliminarly CHIME geochronological study we can draw the following conclusions on the Gyeonggi Massif including the Yeoncheon Group.

(1) The CHIME monazite age for the kyanite-staurolite-garnet schist from the Yeoncheon Group is 255±8 Ma.

(2) The sillimanite-garnet gneiss from the central part of the Gyeonggi Gneiss Complex shows a CHIME monazite age of 245±3 Ma. This suggests that some parts of the Gyeonggi Gneiss Complex formed through the late Permian-early Triassic regional metamorphism.

(3) The ca. 250 Ma metamorphic ages revealed in the Gyeonggi Massif are equivalent to the age for the regional metamorphism in the central part of the Ogcheon Fold Belt in Korea, the Hida Terrane in Japan, and the Qinling-Dabie-Sulu Collisional Belt in China. Presumably, the ca. 250 Ma metamorphism and plutonism took place more widely in East Asia than has been thought.

(4) The ca. 1700 Ma core in a monazite grain from the sillimanite-garnet gneiss in the Gyeonggi Gneiss Complex constrains the sedimentation age of the gneiss protolith to be post-middle Proterozoic.

(5) The two-mica granite intruding the Gyeonggi Gneiss Complex yields a CHIME monazite age of 172±5 Ma.

ACKNOWLEDGEMENTS

We thank Drs. S.J. Choi and K.H. Park at KIGAM for their discussion on the geologic setting and collecting samples, and Mr. S. Yogo of Nagoya University for his excellent technical assistance. One of the authors, D.L. Cho, would like to express his profond thanks to KIGAM and Department of Earth and Planetary Sciences, Nagoya University for providing an opportunity for research.

REFERENCES

Adachi, M., Suzuki, K. and Chwae, U.C. (1996) CHIME age determination of metamorphic rocks in the Ockchon Belt, Korea. *Abstract of the 103rd Annual Meeting of the Geol. Soc. Japan*, 80.

Cho, D.L. and Kwon, S.T. (1994) Hornblende geobarometry of the Mesozoic granitoids in South Kirea and the evolution of crustal thickness. *J. of the Geol. Soc. Korea*, **30**, 41-61.

Cho, M., Kwon, S.T., Ree, J.H. and Nakamura, E. (1995) High pressure amphibolite of the Imjingang belt in the Yeohcheon-Cheongok area. *J. Petrol. Soc. Korea*, **4**, 1-19.

Chwae, U.C., Choi, S.J., Park, K.H. and Kim, K.B. (1996) Explanatory text of the geological map of Cheolwon-Majeonri sheets (scale 1:50,000). Korea Inst. Geol. Mining and Materials, 1-31.

Chwae, U.C., Kim, K.B., Hong, S.H., Lee, B.J., Hwang, J.H., Park, K.H., Hwang, S.K., Choi, B.Y., Song, K.Y. and Jin, M.S. (Compilers) (1995) Geological map of Korea (scale 1:1,000,000). Korea Inst. Geol. Mining and Materials.

Cluzel, D. (1992) Ordovician bimodal magmatism in the Ogcheon belt (South Korea): Intracontinental rift related volcanic activity. *J. Southeast Asian Earth Sci.*, **7**. 195-209.

Cluzel, D., Lee, B.J. and Cadet, J.P. (1991) Indonesian dextral ductile fault system and synkinematic plutonism in the southwest of the Ogcheon Belt (South Korea). *Tectonophysics*, **10**, 131-152.

Dodson, M.H. and McClelland-Brown, E. (1985) Isotopic and paleomagmatic evidence for rates of cooling, uplift and erosion. *Geol. Soc. Mem.*, **10**, 315-325.

Ernst, W.G., Liou, J.G. and Harker, B.R. (1994) Petrotectonic significance of high- and ultrahigh-pressure metamorphic belts: Inferences for subduction zone history. *Int. Geol. Rev.*, **36**, 213-237.

Khan, I.H., Suzuki, K., Shibata, K. and Adachi, M. (1995) Permianc CHIME ages of the Hida Gneiss and early Triassic age of the Mizunami Granite in the Amo area of the Hida terrane, central Japan. *J. Earth Planet. Sci., Nagoya Univ.*, **42**, 31-43.

Lee, S.R. and Cho, M. (1994) Granulite in the Hwacheon-Yanggu area. *Abstract and Program, Geol. Sco. Korea*, 73.

Lee, D.S., Lee, H.Y., Nam, K.S. and Yang, S.Y. (1974) Explanatory text of the geological map of Chucheon sheet (scale 1:50,000). Geol. and Mineral Inst. Korea, 1-9.

Liu, X. (1993) High-P metamorphic belt in central China and its possible eastward extension to Korea. *J. Petrol. Soc. Korea*, **2**, 9-18.

Na, K.C. (1977) The geology and granitization of northeastern Gyeonggi Massif. *Res. Rev. Chungbuk Univ.,* **15**, 57-66.

Na, K.C. (1978) Regional metamorphism in the Gyeonggi Massif with comparative studies on the Yeoncheon and Ogcheon metamorphic belts (I), (on the general geology and petrography of Gyeonggi Massif). *J. Geol. Soc. Korea*, **14**, 195-211.

Na, K.C. and Kim, H.S. (1987) Precambrian Eonothem. In: *Geology of Korea* (ed. D.S. Lee). Geol. Soc. Korea (Kyohaksa Co., Seol), 17-48.

Na, K.C. and Lee, D.J. (1973) Preliminary age study of the Gyeonggi metamorphic belt by the Rb-Sr whole rock method. *J. Geol. Soc. Korea,* **19**, 168-174.

Park, K.H., Lee, B.J., Cho, D.L. and Kim, J.B. (1977) Explanatory text of the geological map of Hwacheon Sheet (scale 1:50,000). Korea Inst. Geol. Mining and Materials (in press).

Ri, J.N. and Ri, J.C. (1990) Geological constitution of Korea. Industrial Publishing House, **6**, 216p.

Ri, J.N. and Ri, J.C. (Editors) (1994) Tectonic map of Korea (scale 1:1,000,000) and explanatory text. Central Geol. Survey, Pyongyang, 22p.

Shibata, K. and Nozawa, T. (1984) Isotopic ages of the Funatsu Granitic Rocks. *J. Japan. Assoc. Min. Pet. Econ. Geol.,* **79**, 289-298.

Smith, H.A. and Barreiro, B. (1990) Monazite U-Pb dating of staurolite grade metamorphism in pelitic schist. *Contrib. Mineral. Petrol.*, **105**, 602-615.

Stern, C.R., Hwang, W. and Wyllie, P.J. (1975) Basalt-andesite-rhyolite-H_2O: Crystallization intervals with excess H_2O and H_2O undersaturated liquidus surface to 35 kilobars, with implication for magma genesis. *Earth Planet. Sci. Lett.*, **28**, 189-196.

Suzuki, K. and Adachi, M. (1991a) Precambrian provenance and Silurian metamorphism of the Tsubonosawa parageiss in the South Kitakami terrane, Northeast Japan, revealed by the chemical Th-U-total Pb isochron ages of monazite, zircon and xenotime. *Geochem. J.*, **25**, 357-376.

Suzuki, K. and Adachi, M. (1991b) The chemical Th-U-total Pb isochron ages of zircon and monazite from the Gray Granite of the Hida terrane, Japan. *J. Earth Sci., Nagoya Univ.*, **38**, 11-37.

Suzuki, K. and Adachi, M. (1994) Middle Precambrian detrital monazite and zircon from the Hida gneiss on Oki-Dogo Island, Japan: their origin and implications for the correlation of basement gneiss of Southwest Japan and Kirea. *Tectonophysics*, **235**, 277-292.

Suzuki, K., Adachi, M. and Kajizuka, I. (1994) Electron microprobe observations of Pb diffusion in metamorphosed detrital monazites. *Earth Planet. Sci. Lett.*, **128**, 391-405.
Suzuki, K., Adachi, M. and Tanaka, T. (1991) Middle Precambrian provenance of Jurassic sandstone in the Mino terrane, central Japan: The Th-U- total Pb evidence from an electron microprobe monazite study. *Sediment. Geol.*, **75**, 141-147.
Yin, A. and Nie, S. (1993) An indentation model for the North and South China collision and the development of the Tan-Lu and Honam fault system, eastern Asia. *Tectonics*, **12**, 801-813.